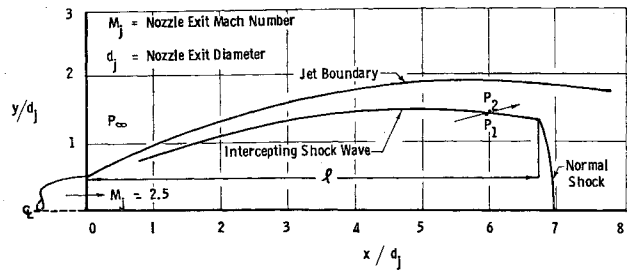

Fig. 1 Exhaust plume for a cold air jet exhausting into still air; $P_j/P_\infty = 12$

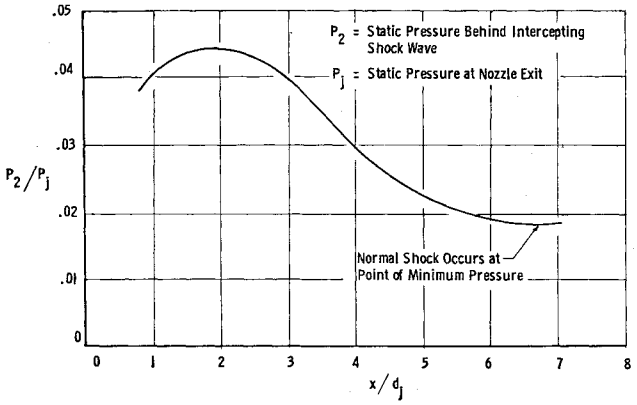

Fig. 2 Variation of the pressure behind the intercepting shock wave for the plume shown in Fig. 1

The characteristics program was used to obtain Fig. 2, which shows a plot of the pressure behind the intercepting shock wave vs x/d_j for the exhaust plume shown in Fig. 1. As can be seen, the pressure first increases and then decreases until an apparent minimum is reached. It is hypothesized that the location of the normal shock wave coincides with the point of minimum pressure. Results from the characteristics program have been compared with existing experimental data, and all results indicate this hypothesis to be correct.

Figure 3 shows a typical comparison of the hypothetical normal shock location with experimental data.[3] Also shown is the predicted normal shock location calculated by applying the method of Adamson and Nicholls[2] to results from the characteristics program. As can be seen, this method predicts that the normal shock will occur at a point further downstream than experimental results indicate. Adamson and Nicholls present a similar curve. However, their curve was obtained using an approximate method to calculate the pressure distribution down the centerline of the exhaust plume. This accounts for the difference between the curve shown in Fig. 3 and the curve shown in Fig. 7c of Ref. 2.

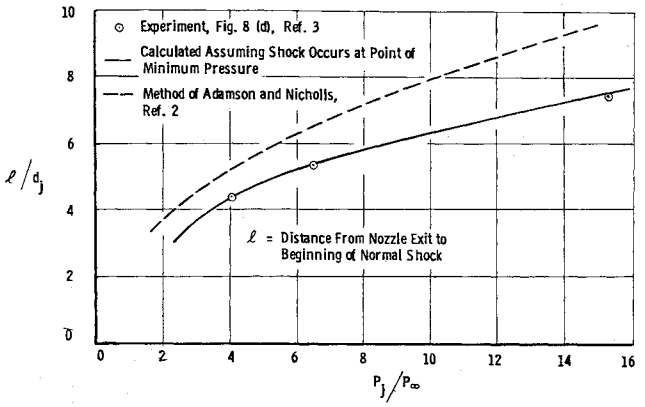

Fig. 3 Comparison of the theoretical and experimental normal shock locations for a cold air jet exhausting into still air; $M_j = 2.5$

Little experimental data for the case of a jet exhausting into a moving external stream are available. However, comparison of available data with results from the characteristics program indicates that the preceding hypothesis also can be used to locate the normal shock for this type flow.

The exact reason for the shock becoming normal, as opposed to striking the axis obliquely, is not known. However, if the normal shock occurs at the point of minimum pressure, there are two important ramifications:

1) The characteristics program assumes inviscid flow, and, therefore, the normal shock is not induced by viscous effects or mixing along the boundary but is determined by the inviscid flow field. Refs. 2, 3, and 5 also reach this same conclusion.

2) The characteristics program is not affected by the flow downstream of the normal shock, and, therefore, the shock location should not be influenced by the flow region behind it. However, Ref. 4 shows that a flame front located behind a normal shock may cause the shock to move upstream.

References

[1] Eastman, D. W., "Two-dimensional or axially symmetric real gas flows by the method of characteristics, Part III: A summary of results from the IBM 7090 program for calculating the flow field of a supersonic jet," Boeing Co. Rept. D2-10599 (1962).

[2] Adamson, T. C., Jr. and Nicholls, J. A., "On the structure of jets from highly underexpanded nozzles into still air," J. Aerospace Sci. 26, 16–24 (1959).

[3] Love, E. S., Grigsby, C. E., Lee, L. P., and Woodling, M. J., "Experimental and theoretical studies of axisymmetric free jets," NASA TR R-6 (1959).

[4] Nicholls, J. A. and Dabara, E. K., "Recent results on standing detonation waves," *Eighth Symposium (International) on Combustion* (Williams and Wilkins Co., Baltimore, Md. 1962), pp. 644–655.

[5] Lord, W. T., "On axi-symmetrical gas jets, with application to rocket jet flow fields at high altitudes," Aeronaut. Research Council Repts. and Memo. R & M 3235 (1961).

Measurements of Thermal Conductivity of Porous Anisotropic Materials

O. E. Tewfik*

Corning Glass Works, Corning, N. Y.

Measurements of the thermal conductivity along several directions and at various average temperature levels of a stainless steel, woven-wire, porous, anisotropic material are described. The material was 0.040-in. thick and was made out of two screens of mesh counts 50 × 250 and 16 × 64 wires/in. by calendering and sintering. Estimated error in the results is ±2%. When compared with the predictions of the thermal ellipse, the results agreed within 1%.

Received by ARS August 27, 1962; revision received January 25, 1963. This paper is a communication from the Heat Transfer Laboratory, Department of Mechanical Engineering, University of Minnesota, Minneapolis, Minn. The author is grateful to K. E. Torrance for taking the thermal conductivity measurements. The woven-wire porous material samples were graciously supplied by Aircraft Porous Media, Glen Cove, N. Y. The research reported in this paper was supported by the U. S. Air Force through the Air Force Office of Scientific Research of the Air Research and Development Command under Contract AF (638)-558.

* Project Engineer. Member AIAA.

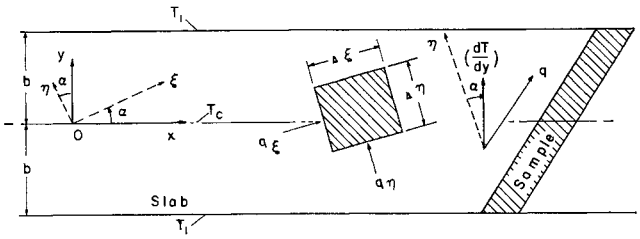

Fig. 1 Anisotropic slab with heat generation

I. Introduction

POROUS materials recently have received considerable attention because of their applications in transpiration cooling. Frequently it is desired to determine the temperature distribution inside such materials, and hence it is necessary to specify the thermal conductivity.

A common type of porous materials is woven from stainless steel wire into a screen. Usually two screens are put one on top of the other and rolled and squeezed between hot calenders. The process results in the sintering of the screen wires at points of contact and also in making the final sheet more compact in one direction than in another. Consequently, the thermal conductivity of the sheet will not be isotropic in general but will depend upon the direction of heat flow. Such anisotropy will be particularly more pronounced if the original screens are woven with different wire counts along their length and width.

In this note, measurements of the thermal conductivity along varied directions and at various temperature levels of a markedly anisotropic sample of a woven-wire porous material are described. The results are compared with the predictions of the thermal ellipse.[1]

II. Method

At any point in an anisotropic material, the heat flux and the temperature gradient have different directions in general. Hence, the thermal conductivity may be defined either as the heat flux divided by the component of the temperature gradient in the direction of the heat flux or as the component of the heat flux in the direction of the temperature gradient divided by the temperature gradient. These two quantities will be denoted by k and k^1, respectively, and in general they have different magnitudes.

Figure 1 shows an infinite slab of anisotropic material of thickness $2b$ in which heat is generated at a uniform rate per unit volume $\dot{q}$ and whose faces are maintained at a uniform temperature T_1. From symmetry, it is seen that the temperature in the slab is a function of the y coordinate only under steady-state conditions, and the temperature gradient has the direction of the y axis. Let the principal axes of conductivity[1] ξ and η make an angle α with the x and y axes, respectively, and the corresponding principal conductivities be k_ξ and k_η, respectively. A heat balance on the indicated volume element results in

$$(k_\xi \sin^2\alpha + k_\eta \cos^2\alpha)\, d^2T/dy^2 = -\dot{q} \qquad (1)$$

From its definition, k^1 can be determined easily in terms of the principle conductivities, and the result is

$$k^1 = k_\xi \sin^2\alpha + k_\eta \cos^2\alpha \qquad (2)$$

Hence Eq. (1) reduces to

$$d_2T/dy^2 = \dot{q}/k^1 \qquad (3)$$

Solving Eq. (3) subject to the boundary condition $T(\pm b) = T_1$ results in the following relation for the centerline temperature T_c:

$$(T_c - T_1) = \dot{q}b^2/2k^1 \qquad (4)$$

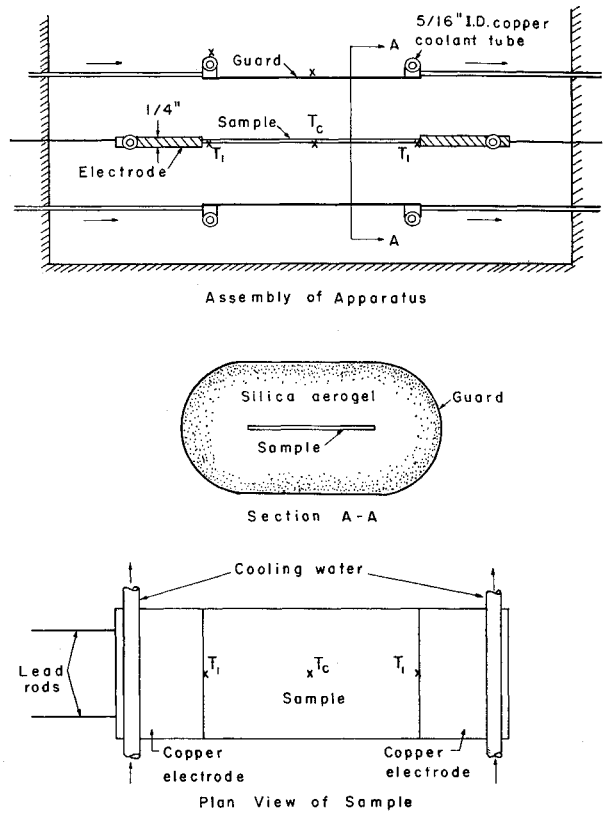

Fig. 2 Thermal conductivity apparatus

If a slice is cut off from the slab in Fig. 1, such that two of its sides are parallel to the direction of the flow of heat, and the other two sides coincide with the isothermal slab faces, neither the temperature field nor the heat flow field will be disturbed, and so the slice can be used as a sample to measure the thermal conductivity along the direction of the temperature gradient from Eq. (4).

III. Apparatus, Measurements, and Discussion

The porous material was made out of two calendered and sintered wire screens of AIST stainless steel type 304 and of mesh counts 50 × 250 and 16 × 64 wires/in. The samples were rectangular sheets, 0.040 in. thick, about 6 in. long, and 2 in. wide. Figure 2 shows the apparatus assembly. Heat was generated in the sample by passing a direct current through it from a Hobart welding generator. Two heavy copper electrodes were soldered to the ends of the sample for electric connections and were cooled by passing two identical streams of water through them.[2] An electrically heated metal guard cylinder was installed around the sample. Its ends were cooled by the same cooling water running through the sample electrodes. The power input to the guard cylinder was adjusted until the temperature in its middle point matched that of the sample middle point within about 0.2°F. Moreover, the space between sample and guard cylinder was filled with silica aerogel, and the assembly was placed in a box surrounded by aerogel on all sides. Thus the heat exchange between the sample and the surroundings (other than the electrodes) is negligible.[2]

The apparatus was calibrated by measuring the conductivity of a lead sample of 99.99% purity. The results agreed within ±1% with the International Critical Tables.

Next the thermal conductivity of the porous material was measured. The ξ axis was chosen arbitrarily along the direction of the wires of count 64/in. in the coarse side of the sample. The principal conductivities k_ξ and k_η were determined first at various average temperature levels defined as $(T_1 + T_c)/2$. The rest of the porous samples were cut such

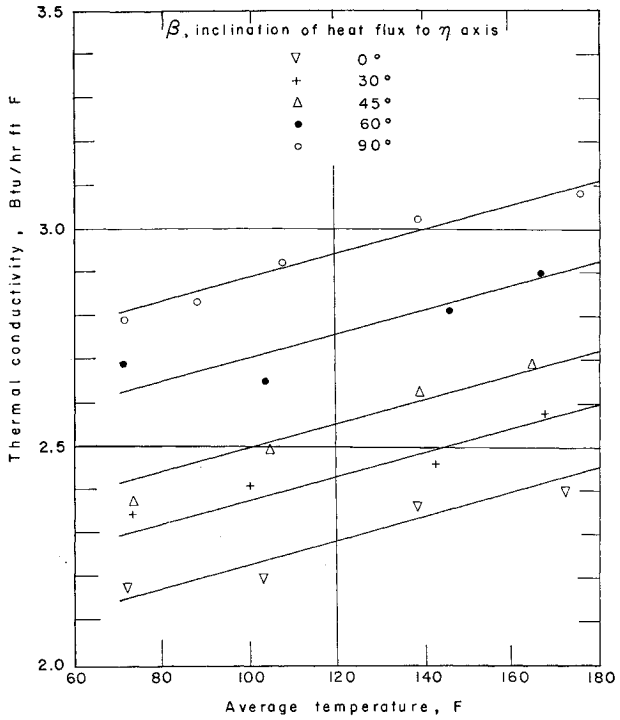

Fig. 3 Thermal conductivity for five various directions

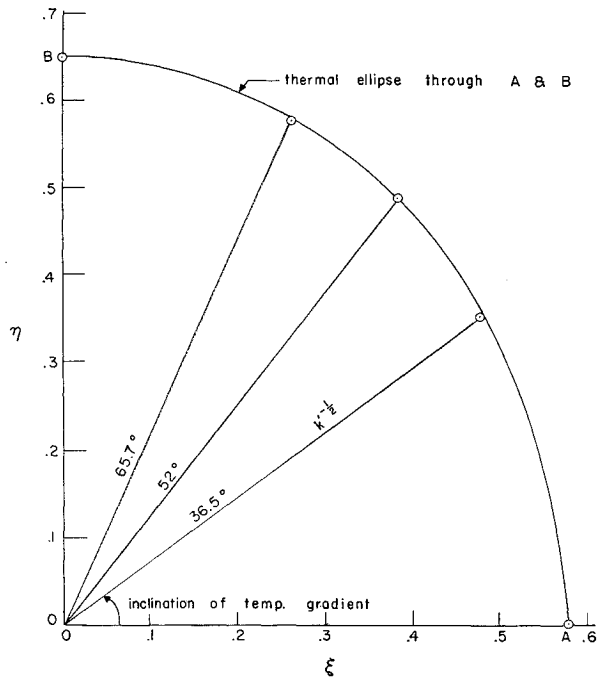

Fig. 4 Variation of thermal conductivity along the temperature gradient with direction for woven wire material 12 × 64/250 × 50

that their longer sides make angles of 30°, 45°, and 60° with the η axis. These are also the inclinations of the heat flux in the respective samples, since heat is supposed to flow parallel to the longer sides of the sample (Fig. 1). With the direction of the heat flux now known relative to the principal axes of conductivity, the direction of the temperature gradient was computed for each sample. The electrodes then were machined so that their edges were normal to the direction of the temperature gradient and then soldered to the sample. The thermal conductivity was measured at various average temperature levels, and the results are plotted in Fig. 3. The error in measurement is estimated to be ±2%.

Dividing Eq. (2) by k^1 results in

$$1 = (k_\xi/k^1) \sin^2\alpha + (k_\eta/k^1) \cos^2\alpha \qquad (5)$$

If at any point in the sample a radius vector of length $(k^1)^{-1/2}$ is measured along the direction of the temperature gradient, the locus of the tip of the radius vector relative to the principal axes of conductivity will be given by

$$1 = k_\xi \cdot \xi^2 + k_\eta \cdot \eta^2 \qquad (6)$$

Equation (6) represents an ellipse with semi-axes of lengths $k_\xi^{-1/2}$ and $k_\eta^{-1/2}$ along the ξ and η axes, respectively. This ellipse is called the thermal ellipse and is drawn in Fig. 4 with its principal axes computed from the measured values of k_ξ and k_η. The directions of the temperature gradient in the various samples also are indicated. Along each, a length is measured equal to $(k^1)^{-1/2}$, where k^1 is the respective thermal conductivity taken from the faired curves in Fig. 3 at 120°F. The experimental points deviate by less than 1% from the thermal ellipse. Thus the method of measuring thermal conductivities of metals in the form of a thin sheet by heat generation, originally expounded for thin walled tubes[3] and extended here to the case of anisotropic materials, seems to be a satisfactory as well as a convenient method.

References

[1] Carslaw, H. S. and Jaeger, J. C., *Conduction of Heat in Solids* (Oxford University Press, Oxford, England, 1948), 1st ed., p. 28.

[2] Johnson, B. V., "Heat transfer from a cylinder in crossflow with transpiration cooling," M. S. Thesis, Univ. Minnesota (1960).

[3] Allen, R. W., "Measurements of friction and local heat transfer for turbulent flow of a variable property fluid (water) in a uniformly heated tube," Ph.D. Thesis, Univ. Minnesota (1959).

Recovery of Water or Oxygen by Reduction of Lunar Rock

BRUCE B. CARR*

Callery Chemical Company, Callery, Pa.

The production of water or oxygen on the moon is considered from a process viewpoint. Although water would be the most desirable raw material, the actual requirement for either life support or propellant use is primarily oxygen, based on weight of material required. Since almost half the weight of the moon must be oxygen, there can be no doubt about the supply available. Several processes are considered for producing water or oxygen on the moon. The approach suggested is not dependent completely on our knowledge of moon composition, and yet it can take advantage of the optimum raw material, water, if it can be found. Processes considered vary in technological difficulty from simple rock dehydration to reduction of silicates, the objective being maximum simplicity of operation even at a cost of increased power requirement and technical problems. The criteria of weight payout time is suggested for process evaluation. This is the time required to produce a weight of product equal to the weight of plant required. A weight payout time of

Presented at the ARS 17th Annual Meeting and Space Flight Exposition, Los Angeles, Calif., November 13–18, 1962; revision received February 5, 1963.

* Senior Engineer.